

MICROWAVE SCREEN WITH MAGNETICALLY CONTROLLED ATTENUATION

S. N. Starostenko and K. N. Rozanov

Institute for Theoretical and Applied Electromagnetics
Russia

Abstract—The effect of magnetic bias on dielectric spectra of composite sheets filled with Fe or Co-based microwires is studied experimentally and via simulation. The permittivity is measured using a free-space technique within the frequency band from 6 to 12 GHz. The bias is applied either parallel or perpendicular to the microwave electric field; the bias strength varies from 0 to 2.5 kOe. The composites with Fe-based wires reveal a single region of bias dependent permittivity under bias about 800–1000 Oe. The composites with Co-based wires reveal two such regions: the high-field region is close to that of composites with Fe wires, and the low-field region corresponds to the coercive field of Co wires (2–3 Oe). The high-field effect is related to the dependence of ferromagnetic resonance (FMR) parameters on bias; the low-field effect is related to the rearrangement of the domain structure of Co-based wires. The interference of magnetoimpedance and dipole resonance is analyzed, revealing the effects off wire length, diameter, parameters of magnetic resonance and composite structure. The results are considered in view of application to the problem of controlled microwave attenuation. Simulation shows that the narrower is the FMR spectrum and the higher is the admissible loss of a sheet in a transparent state, the wider is the dynamic range of attenuation control. The attenuation range of a lattice of continuous wires is smaller than that of a screen with identical wire sections, where the magnetoimpedance effect is amplified resonantly. At 15 GHz frequency the strength of the bias switching opaque sheet with Fe-based wires to the transparent state is about 2000 Oe. For 3 dB admissible loss, the range of attenuation control about 10 dB is feasible in a composite with aligned wire sections. If the aligned sections are distributed regularly, the loss in a transparent state is about 1 dB lower.

Corresponding author: S. N. Starostenko (snstar@mail.ru).

1. INTRODUCTION

Attempts to synthesize an adaptive material with controlled microwave properties, particularly attenuation, have a long history. For example, pin diodes are proposed for the design of adaptive radar absorbers [1, 2] and tunable frequency selected surfaces [3, 4]. Other principles of the design of tunable microwave materials, such as ferroelectrics [5] and conducting polymers [6] controlled by electric field, or ferromagnetic materials controlled by magnetic field [7], are also considered for free-space applications.

We consider an absorbing screen of a diluted polymer-binded mixture filled with sections of permeable wires. The theory of permittivity control in composites filled with glass-coated microwires of permeable amorphous alloys is suggested in [8–10]. The idea is that the penetration depth (skin-depth) δ and consequently the surface impedance of a permeable wire depend at microwaves on both direct current (d.c.) conductivity and complex permeability μ . The wire impedance defines the composite permittivity and consequently the screen attenuation. The wire permeability μ is a function of the strength H_{ext} of external magnetic bias. Therefore the surface impedance also depends on H_{ext} . At megahertz frequencies the effect is so high that it is called the giant magnetoimpedance (GMI) effect [11, 12]. The development of a large tuned screen seems promising for various practical applications, as the tuning bias should be small enough to be applied by passing a current through a wire mesh [10].

It may seem that the attenuation may be controlled more directly through the microwave permeability of a wire-filled composite. It is not so because the composite is too diluted: even the anisotropic sample of closely packed sections of amorphous wire (the filling factor is as high as 0.7) exhibits microwave permeability that is close to unity [8]. The reason is that the magnetization perpendicular to wire axis is negligible due to high demagnetization factor. The major contribution to permeability has the magnetization along the wire, but the longitudinal magnetization has low resonance frequency.

Practicable wire-filled composites are usually isotropic as they are filled with randomly oriented fiber sections. The fiber-filled mixtures display that the lower is the percolation threshold, the more elongated are the inclusions [13]. It means that the fibers intertwine into felt, and it becomes impossible to increase the filling factor further. Therefore the practicable wire-filled composites are hundredfold more diluted than samples with closely packed wires and are expected to have microwave permeability equal to unity.

Below, we analyze the feasibility of a composite screen with the

microwave parameters controlled by external action that can be applied to a sheet sample without any circuitry. Particularly we consider the absorbing screen of a diluted polymer-bound mixture filled with glass-coated fibers of permeable metal, study the effect of magnetic bias on permittivity spectrum and estimate the range of transparency and reflectivity control by magnetic bias. Contrary to studies on response of a single wire [15–17], or lattice of thin continuous wires [15, 18] we consider the practicable composites, namely the mats filled with wire sections. The absorption region of the composite is limited by the wire length within approximately 2 ÷ 30 GHz range as the long wires intertwine, while the properties of short ones are unstable [8, 18].

The dielectric spectra of composites under study are more complicated than that of the samples with impermeable wires [13]. The spectra are similar to that of effective permittivity obtained for a single wire stretched across the section of a coaxial line [15] and consist of two separate absorption peaks affected by magnetic bias. The formation of two peaks of absorption is explained by the interference of the resonance of a wire dipole and of the current-induced ferromagnetic resonance (FMR) of circumferential permeability and is validated numerically. The wire length fixes the dipole resonance, while the FMR frequency is controlled by magnetic bias.

The measurements reveal two different mechanisms of magnetocapacitance (bias-on-permittivity) effect. The weaker effect takes place at bias equal to coercive field and can be attributed to the rearrangement of domain structure in magnetically bistable wire. The stronger effect is observed for a fixed domain structure and is related to the dependence of FMR parameters on the external bias H_{ext} .

The aim of the article is to determine the optimal parameters of a tunable microwave screen filled with permeable wires. That is to find the optimal length and thickness of the wire sections, filling factor, structure and the thickness of the screen designed to be transparent at a specified operating frequency and to relate the bias strength to the dynamic range of attenuation control at this operating frequency.

The theoretical analysis allows numerical comparison of the control range of the plane-isotropic screen studied experimentally and of anisotropic structures of the same constituents. Namely, we compare the properties of the composite of randomly distributed aligned Fe-based wire sections, of the lattice of regularly distributed aligned wire sections, of the mesh of continuous parallel wires and of the plane-isotropic composite.

2. EXPERIMENTAL TECHNIQUE

The samples under study are obtained by coprecipitation of glass fiber and wire sections in a diluted solution of polystyrene. The composite mats are 1.2 mm thick and have the density about 0.7 g/cm^3 . The permittivity ε_h of a mat without wires is about 1.2.

The sections are cut of two different types of glass-coated amorphous wires with precision of about $\pm 0.1 \text{ mm}$. The section length varies from 7 to 10 mm for different samples. As the wire length exceeds the sample thickness, the samples are plane-isotropic (the wire sections have two dimensional orientation). The permeable core is of either Co-based amorphous alloy with diameter $d = 5 \mu\text{m}$ and conductivity σ about $20000 \text{ Ohm}^{-1}\text{cm}^{-1}$ or Fe-based amorphous alloy FeSiBMnC with $d = 4 \mu\text{m}$ and conductivity about $70000 \text{ Ohm}^{-1}\text{cm}^{-1}$. To exclude the contribution of contacts, the conductivity is calculated from the measured resistance of wire sections of several lengths. The volume fraction p of permeable alloy in composite sheets is about 0.008%. The external diameter of glass shell for wires of both types is about $15 \mu\text{m}$. The shell and core diameters are measured with optical microscope.

The complex permittivity ε is measured within 6–12 GHz frequency band using the free-space sliding short method [13]. The value of complex permittivity is found by fitting procedure that minimizes the least-squares discrepancy between the measured and calculated scalar reflectivity data. To yield reliable permittivity data, the fitting procedure treats 10–12 reflection coefficients obtained for different gaps between the sheet sample and metal short. The sample is irradiated by the normally incident wave from a horn antenna.

The measurements are performed under two bias orientations relative to the polarization of irradiating microwave. The bias strength H_{ext} varies from 0 to 2.5 kOe with either 0.5 kOe step or with gradual sweep.

3. EXPERIMENTAL RESULTS

The composites with resistive fibers, such carbon fibers, have a simple Debye-type dielectric spectrum consisting of a single relaxation line of absorption. The fiber resistance and length define the relaxation time. If the resistance of wire section is small, long wire of an ideal conductor in a free space the absorption maximum takes place at the frequency of dipole resonance (about 15 GHz). The linear resistance of the wires under study is as high as 500 Ohm/cm , so the absorption spectrum of a composite should be almost as wide as the Debye absorption.

The permittivity measurements show (Fig. 1) that high dielectric

losses are indeed observed within the whole experimental frequency range. However, contrary to spectra of composites with unpermeable fibers [13,20] the absorption spectra of composites under study are more complicated. They reveal two separate absorption maxima located near the ends of the experimental frequency range (see Fig. 1). The formation of separate absorption maxima occurs due to the sharp increase of wire resistance at the FMR frequency (see Section 4). The narrower is the FMR spectrum, the more distinctive should be the separation of absorption maxima. The zero bias permittivity spectra are more diffused than expected (compared with Fig. 1(b), and Fig. 6 minds the different scales of simulated and experimental graphs).

In practice, the external bias affects both the FMR frequency and effective damping factor. The higher is the bias strength, the smaller is the relative difference in local fields, and hence the narrower becomes the FMR spectrum [21]. We observe that the broad absorption spectra are resolved into two separate lines under 1 kOe bias despite the contribution of the less magnetized wires that are non-parallel to bias (compare the black and gray lines in Fig. 1).

The more significant difference in the microwave behavior of Fe- and Co-based wires is observed under fixed-frequency measurements of permittivity as a function of bias (Figs. 2 and 3). The Co-based samples exhibit two regions of bias-dependent permittivity for both bias orientations due to the contribution of the wires tilted to the

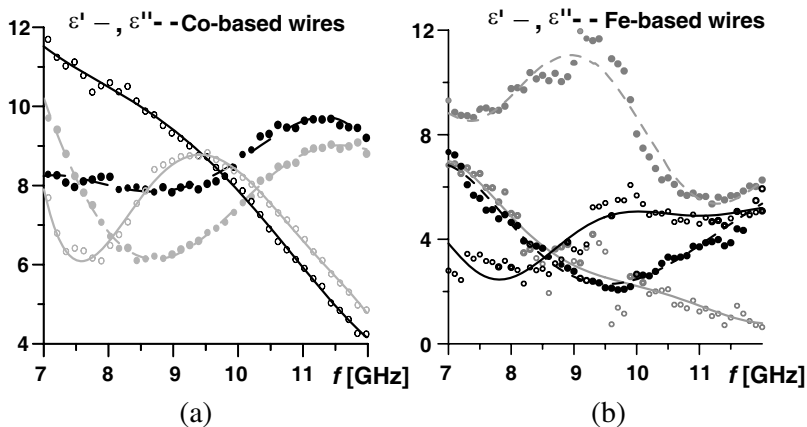


Figure 1. Permittivity spectra of samples filled with 10 mm-long: (a) Co-based wires; (b) Fe-based wires. The black lines correspond to zero bias, the gray ones correspond to 1 kOe bias applied parallel to the microwave electric field.

microwave electric field (Fig. 2).

The first region appears at bias strength about $2 \div 3$ Oe. The permittivity change $\Delta\varepsilon$ is small here; therefore it is difficult to determine the shape of the absorption line. The data in Fig. 2 are obtained under gradually varying bias (about 1 Oe/sec), and we

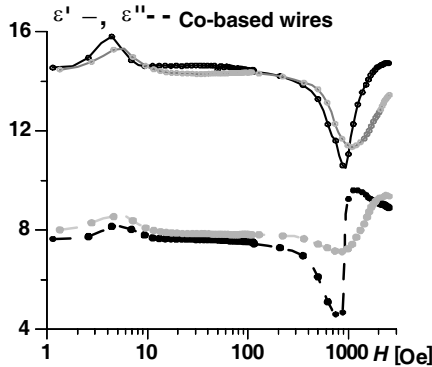


Figure 2. Permittivity as bias function for the sample with Co wires ($f = 6$ GHz, $L = 10$ mm).

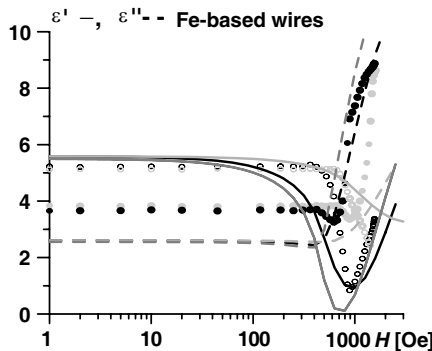


Figure 3. Permittivity as function of bias for the sample with Fe-based wires ($f = 10.4$ GHz, $L = 10$ mm). The experimental data are presented by dots, the simulation data (see Section 5) are presented by continuous lines. The black dots and lines correspond to bias applied parallel to the microwave electric field $H_{ext} \parallel E$; the gray dots and lines correspond to perpendicular bias $H_{ext} \perp E$. The light-gray and black lines correspond to randomly oriented wires; the dark-gray lines correspond to wires aligned parallel to E .

attribute the permittivity change under low bias to the process of rearrangement of domain microwave field. Similar permeability effect has been observed in composites with CrO_2 [22], where the microwave permeability changes under sweeping bias. The effect of final magnetic textures (of eventual domain structures) on the permeability spectra of CrO_2 composites is negligible.

Another change in permittivity appearing under high bias is related to the shift of FMR frequency similar to the effect observed in Fe-based wires (Fig. 3). The similarity of black and gray graphs in Figs. 2 and 3 indicates the high contribution of the wire sections inclined to the microwave electric field, though the peak of dielectric absorption is approximately twice higher and sharper if the bias is parallel to electric field.

The sample with Fe-based wires exhibits (dots in Fig. 3) higher dielectric losses and sharper manetocapacitance effect than expected (simulated curves in Fig. 3) for a plane-isotropic screen. It is easy to see the compared data in Fig. 2 and Fig. 3 that the FMR frequency of Fe-based wires is higher than that of Co-based ones. As the microwave screen with Fe-based wires can operate at higher frequency and under lower bias; the range of transparency control ΔT is investigated for composites with the Fe-based wires.

The transmission coefficient T is measured for a 1 mm thick sample at the frequency close to that of FMR, where the skin-depth is minimal

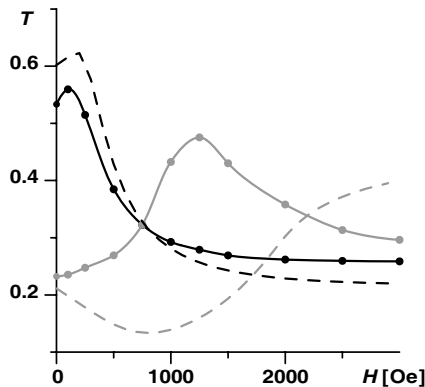


Figure 4. Power transmission as function of parallel bias for the sample with Fe-based wires ($L = 10$ mm, $f = 10$ GHz and $f = 15$ GHz, black and gray lines correspondingly). The dots connected by solid lines present the experimental data, while the dashed curves present the results of simulation (see Section 5).

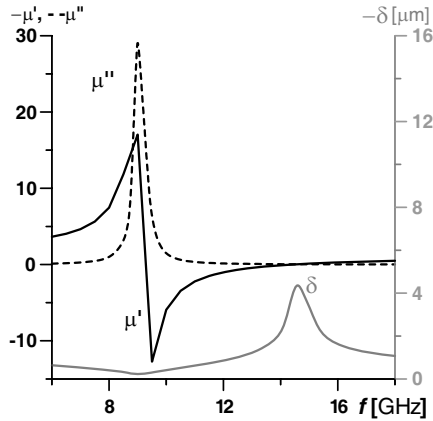


Figure 5. Reconstructed frequency dependence of permeability (solid and dashed black lines) and skin-depth (solid gray line) for FeSiBMnC microwire with $\mu_{st} = 2.5$, $\Gamma = 0.04$, $\sigma = 70000 \text{ Ohm}^{-1}\text{cm}^{-1}$ and $H_a = 3.25 \text{ kOe}$.

and at the frequency close to that one where the skin depth is expected to be maximal (about 10 and 15 GHz correspondingly, see Fig. 5).

At 10 GHz the experimental data in Fig. 4 are in good agreement with theoretical estimations (see Section 5), while at 15 GHz the transparency change is higher than expected. Moreover, the transparency maximum at 15 GHz is reached under 1 kOe bias contrary to expected 3 kOe (compare the continuous and dashed lines in Fig. 4).

The range of attenuation control presented in Fig. 4 significantly exceeds the range expected due to GMI [10, 25], and it can be increased further for the same wires, as the sample under study is not optimal from the viewpoint of its structure and composition.

4. COMPUTATION OF PERMITTIVITY AS THE FUNCTION OF FREQUENCY AND BIAS FOR ANISOTROPIC COMPOSITES

To estimate the limits of attenuation control at a given operating frequency, we have to calculate the bias-affected reflection and transmission coefficients of a plane screen of optimal for this frequency thickness and composition. The operating frequency cannot be arbitrary, as it is located in the vicinity of FMR frequency of the available permeable wire. Below we estimate the properties of a screen filled with Fe-based wires, as their magnetocapacitance effect (Fig. 3) exceeds that of Co-based ones (Fig. 2).

The reflection R and transmission T coefficients of a plane sample depend on its complex permittivity ε (in case under study $\mu \approx 1$) and thickness [23]. Considering the permittivity of a diluted composite filled with insulated metal inclusions we generalize the approach [13] to microwave absorption of a matrix mixture upon the mixture with elongated magnetoresistive ellipsoids. Applying Maxwell-Garnett mixing formula (1) we can calculate the complex permittivity of an anisotropic composite filled with aligned wire sections:

$$\varepsilon_{mix} = \varepsilon_h \left[1 + \frac{(\varepsilon_{sec} - \varepsilon_h) p}{(1 - p) N (\varepsilon_{sec} - \varepsilon_h) + \varepsilon_h} \right] \quad (1)$$

Here $\varepsilon_h \approx 1.2$ is the binder permittivity; N is the depolarization factor of the wire of length L and diameter d ; p is the volume fraction of wire sections of permittivity ε_{sec} . The latter is to be determined as follows.

We treat the wire as a complex dielectric with effective permittivity ε_{eff} . In case under study, the section length L is not negligible compared to the operating wavelength λ . Therefore, the wire inclusion cannot be implicitly characterized as a small ellipsoid by the shape-dependent factor N in Equation (1). The relatively long ($L/\lambda > 0.1$) wire is a dipole. Calculating the complex permittivity ε_{sec} of a dipole, we consider the serial connection of all constituents (capacitive, inductive and resistive) of dipole admittance. The first item in denominator of relation (2) corresponds to capacitive resistance of a dipole; the second one corresponds to its inductance (see [13, 18]), while the third item corresponds to pure resistance of the wire. If the aligned dipoles are distributed randomly, we should add to the third item the radiation loss $R_{rad} = 75 \text{ Ohm}$ [13]. As a result, the effective permittivity of the wire section ε_{sec} depends on the properties of the wire as well as on the section length and distribution of sections in matrix:

$$\varepsilon_{sec} = \frac{\lambda^2}{\frac{\lambda^2}{\varepsilon_{eff}'} - \pi d^2 \ln\left(\frac{L}{d}\right) + i \left(\frac{\lambda^2}{\varepsilon_{eff}''} + \frac{\pi^2 c \varepsilon_{vac} \lambda d^2}{2L} R_{rad} \right)} \quad (2)$$

where λ is the wavelength; $c = 3 \times 10^8 \text{ m/sec}$ is the light velocity; $\varepsilon_{vac} = 8.85 \times 10^{-12} \text{ F/m}$ is the dielectric constant; ε_{eff} is the effective permittivity of the infinitely long wire.

Note that ε_{eff} of an inclusion of complex dielectric depends, in general case, on both frequency and inclusion size even if the latter is much smaller than the wavelength. The effect of inclusion size upon the microwave permittivity of a composite becomes significant if the inclusions are electrically thick [13] (the smallest dimension of inclusion is comparable or higher than the penetration depth δ).

If the metal wire of d.c. conductivity σ is very thin ($d \ll \delta$), the imaginary part of its permittivity ε'' is proportional to the wavelength λ while the real part ε' is about unity:

$$\varepsilon = 1 - i\sigma\lambda/2\pi\varepsilon_{vac}c \quad (3)$$

If the wire is thick enough ($d \geq \delta$), we have to take into account that the effective conductivity σ is frequency-dependent as it is the function of penetration depth. It is well known that the penetration depth of a magnetic material depends on both complex permittivity $\varepsilon = \varepsilon' - i\varepsilon''$ and permeability $\mu = \mu' - i\mu''$. Therefore, the effective permittivity ε_{eff} of a long permeable wire parallel to the microwave electric field is calculated taking into account the penetration depth in the infinite cylinder with both magnetic and dielectric losses [24, 25]:

$$\varepsilon_{eff} = \frac{\varepsilon J_1(2\pi d\sqrt{\varepsilon\mu}/\lambda)}{J_0(2\pi d\sqrt{\varepsilon\mu}/\lambda) 2\pi d\sqrt{\varepsilon\mu}/\lambda - J_1(2\pi d\sqrt{\varepsilon\mu}/\lambda)} \quad (4)$$

Here J_0 and J_1 are Bessel functions; μ is the circumferential permeability of metal wire; permittivity ε is defined by (3). Note that in the vicinity of FMR the frequency dependence of complex permittivity ε_{eff} for a wire of permeable metal differs significantly from that of impermeable one.

To obtain the FMR parameters and $\mu(f)$ we consider the simplest model of a single-domain inclusion with uniaxial anisotropy where the bias and anisotropy fields are parallel. In this case, the FMR spectrum has the Lorentzian shape described by Equation (5) similar to derived in [26]:

$$\mu = 1 + \frac{(\mu_{st} - 1)/(1 + H_{ext}/H_A)}{1 - \left[\frac{2\pi f}{\gamma(H_A + H_{ext})} \right]^2 + i \frac{2\pi f\Gamma}{\gamma(H_A + H_{ext})}} \quad (5)$$

where $\gamma = 2.8 \text{ GHz/kOe}$ is the gyromagnetic factor for Fe; μ_{st} is the quasistatic (low-frequency) permeability under zero bias ($H_{ext} = 0$); H_a and H_{ext} are the anisotropy and the external bias fields correspondingly; Γ is the damping factor; f is the frequency.

Equation (5) describes the quasi-bulk permeability of metal that defines the penetration depth together with its bulk conductivity, inclusion shape and orientation (4). Equation (5) is easy to comprehend taking into account that the longitudinal demagnetizing factor is close to zero as $L \gg d$ and that the induced current magnetizes the wire circumferentially with demagnetizing factor also equal to zero. The approach is justified at least for the Fe-based wires with positive magnetostriction where the domains are magnetized mostly axially. The fraction of domains magnetized perpendicularly to the axis is small [19].

According to the data in Fig. 1(b) the FMR frequency of the wire is about $F_{rez} \approx 9.2$ GHz, but for quantitative estimations we need all parameters of FMR spectrum. We reconstruct the FMR spectrum treating the data [17] on the conductivity of a similar Fe-based wire as a function of frequency.

The spectrum of circumferential permeability $\mu(f)$ displayed in Fig. 5 is reconstructed by fitting parameters of Equation (5) to minimize the discrepancy of the effective conductivity $\sigma_{eff} = 2\pi f \varepsilon_{vac} \varepsilon_{eff}''$ calculated using Equation (4) from that of the measurements [17]. The fitted parameters of permeability spectrum (Fig. 5) are as follows: $\Gamma = 0.04$; $\mu_{st} = 2.5$; $H_a = 3.25$ kOe.

The zero-bias FMR frequency F_{rez} for these parameters is equal to 9 GHz, which is close to 9.2 GHz estimated from data in Fig. 3. The product of static permeability and resonance frequency $(\mu_{st} - 1) \times F_{rez} \approx 13.5$ GHz calculated using Equation (5) is lower than Snoek's limit, which is about 40 GHz for pure iron. The difference may be attributed to dilution of iron, as the FeSiBMnC amorphous alloy is a solid solution. The value of damping factor is typical for glass-coated wires [16, 27]. The penetration depth δ in Fig. 5 is calculated based on the reconstructed permeability (5) and permittivity of the infinite wire (3).

If the wire permeability is frequency independent (the well known particular case of an impermeable alloy), the penetration depth decreases with frequency as $\delta(f) \sim 1/\sqrt{f}$. In case of a permeable metal, the function $\delta(f)$ is more complicated and depends on the shape of FMR spectrum.

In case of the Lorentzian shape of the line of magnetic absorption (5), it is easy to derive that there are two extremums of $\delta(f)$ function. Namely, the skin-depth δ is minimal $\delta_{min} = 1/\sqrt{2\pi F_{rez} \sigma \mu_{vac} (\mu_{st} - 1)}$ at the FMR frequency F_{rez} , and δ is maximal $\delta_{max} = 1/\sqrt{\sigma \mu_{vac} \pi f (|\mu| + \mu'')}$ at the frequency where $(|\mu| + \mu'')$ is minimal. Here $\mu_{vac} = 1.25 \times 10^{-6}$ Hn/m is the magnetic constant. The minimal skin-depth δ corresponds to the highest relative resistance of the wire and vice versa.

It is important that these very extremums of penetration depth specify the maximal change of wire impedance and consequently define the optimal parameters of a tunable screen, namely the composition, operating frequency, necessary bias strength and obtained range of attenuation control. The frequency of δ_{min} is within the limits of experimental frequency range and is determined relatively accurately; consequently we have a good agreement between the experimental and

simulated data at 10 GHz (Figs. 3 and 4). The frequency of δ_{\max} is estimated assuming the Lorentzian shape of FMR spectrum. The comparison of the experimental and simulated transmission data at 15 GHz (Fig. 4) shows that the estimated value exceeds the actual frequency of δ_{\max} .

Note that under $H_{ext} = 0$ the wire resistance $\rho_{eff} = 1/\sigma_{eff} = 1/\sqrt{2\pi f \varepsilon_{vac} \varepsilon_{eff}''}$ is minimal at 14.4 GHz, while under $H_{ext}=1.8$ kOe the resistance is maximal. The magnetoimpedance curve at 14.4 GHz is shown further in Fig. 8; the impedance change here requires high bias, but the change is about four times higher than that due to GMI [25].

To obtain the permittivity close to the measured values ($\varepsilon' \approx 12$), the volume fraction p in Equation (1) is expected to be twice smaller than the filling factor for the manufactured plane-isotropic samples, where the wires are not aligned. The calculation produces the value $p \approx 0.0026\%$ that is about 3 times lower than the filling factor of the samples under study. The discrepancy can be attributed to the wire sections nonparallel to the plane of the sheet and to distortion of wire properties at the section ends [22].

At last, based on the spectrum of circumferential permeability for Fe-based wire (Fig. 3), wire conductivity ($70000 \text{ Ohm}^{-1} \text{ cm}^{-1}$), length ($L \approx 1 \text{ cm}$) and core diameter ($d = 4 \mu\text{m}$), we can calculate the permittivity spectra of a composite under bias of given strength (Fig. 6). These spectra are the result of the interference between the wire-dipole resonance and the current-induced resonance of circumferential permeability (magnetoimpedance resonance). The spectra in Fig. 6 illustrate the transformation of the effective permittivity spectra from a resonance type to a relaxation one due to GMI in the vicinity of the antenna resonance [10]. But in the case under study, the interference of antenna resonance and impedance resonance is optimized. As a result, the Debye absorption corresponding to high-impedance state of the wire is transformed into two lines, and the total permittivity change is significantly higher than that due to GMI effect [10].

The highest change of the wire resistance is observed at the frequency about 14.5 GHz, where the skin depth reaches its maximum under zero bias (see Fig. 5 and Fig. 8). At this frequency, the wire has minimal effective resistance, and the absorption line has the minimal width (black lines in Fig. 6). The second absorption peak at about 8.5 GHz has the relaxation nature (the real part of wire resistance is much higher than the inductive one), as at this frequency the wire resistance is maximal due to zero-bias FMR. At the same time, the deviation from FMR frequency abruptly decreases the wire resistance and makes the absorption line much sharper than the relaxation

(Debye) line.

The wire resistance reaches maximum under 2 kOe bias that shifts the FMR spectrum to 14.4 GHz (see Figs. 5 and 8). Under this bias the absorption exhibits the relaxation nature similar to absorption in an RC circuit. The losses are minimal because the wire resistance is too high (dark-gray lines in Fig. 6). The frequency deviation from the peak of FMR spectrum results in the decrease of effective resistance and leads to formation of two separate lines of dielectric absorption. The further increase of bias strength again decreases the wire resistance at 14.4 GHz and increases the ε'' value. Under 4 kOe bias, the wire permeability within the investigated frequency band is close to unity, but the effective resistance is higher than in the case of maximal skin-depth. Therefore, the absorption peak has lower frequency (about 12.5 GHz), and the absorption line is much wider than in the case of minimal resistance (compare the black and light-gray curves in Fig. 6).

The two-line shape of permittivity spectra in Fig. 6 resembles the spectra for a FeCoSiB microwire stretched across a coaxial line [15], although the magnetocapacitance effect is much stronger in the case under study. The reason is that in [15] the frequency of dielectric resonance (~ 1 GHz) is lower than the FMR frequency (there are no data on the wire permeability in [15], but we suppose from the permittivity spectra that the peak of magnetic loss takes place at ~ 2 GHz). Therefore, the step of wire impedance takes place at a shoulder of absorption curve, where its effect on the permittivity

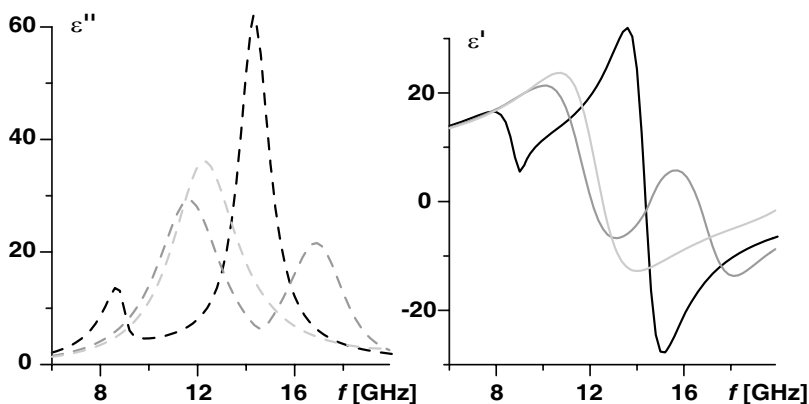


Figure 6. Permittivity ε' and ε'' (continuous and dashed lines) dispersion curves under bias $H = 0, 2, 4$ kOe (black, dark-gray and light-gray curves correspondingly) of a composite containing 2.7×10^{-3} vol% Fe-based wire sections 8 mm-long.

is small. In case of the samples under study, the frequency of dielectric absorption is tuned to be equal to the frequency of minimal wire impedance. Therefore, the magnetoimpedance effect on the permittivity is resonantly increased.

The composition and structure of the optimized screen differs from that of the samples studied experimentally. To obtain the widest range of attenuation control we have to tune the length of the wire section to the operating frequency (14.5 GHz in Fig. 6) and to align the sections parallel to electric and bias fields. The discrepancy between the calculated and experimental dispersion curves (Figs. 1 and 6) is mainly the result of the simplified model that assumes the Lorentzian FMR spectrum and considers the idealized structure with parallel wires.

5. COMPARISON OF THE ATTENUATION RANGE FOR PARTICULAR SCREEN STRUCTURES

To take into account the random orientation of wire sections in the measured sample we need to consider the effective magnetizing field as the function of the angle α between the wire axis and bias field: $H_{eff} = H_A + H_{ext} \cos \alpha$. To simplify calculations we neglect the contribution of domains that are magnetized perpendicular to the wire axis. We assume that the wire remains magnetized axially independently on bias orientation because the demagnetizing factor perpendicular to the wire axis is equal to zero. Therefore, to describe the circumferential permeability as the function of the angle α between the wire axis and the bias field we have to substitute H_{ext} in Equation (5) by $H_{ext} \cos \alpha$ in case of a perpendicular bias H_{ext} is replaced by $H_{ext} \sin \alpha$.

Note that under zero bias the conductivity of wires is independent of their orientation, while under non-zero bias the circumferential permeability and consequently the wire conductivity is the function of the angle α between the wire axis and bias. Therefore, we consider the electric polarization of the wires as the function of the same angle α between the wire axis and the microwave electric field. As a result, we modify Equation (1):

$$\varepsilon_{mix} = \varepsilon_h \left[1 + \int_0^{\pi/2} \frac{[\varepsilon_{wire}(\alpha) - \varepsilon_h] p \cos^2 \alpha}{(1 - p \cos^2 \alpha) N [\varepsilon_{wire}(\alpha) - \varepsilon_h] + \varepsilon_h} d\alpha \right] \quad (6)$$

Using (1), (6) and the modified Equation (5) we obtain the curves that resemble the experimental dependence of permittivity on bias (see the black curves and dots in Fig. 3)

The discrepancy between the calculated permittivity for plane-isotropic sample and experimental data (the experimental permittivity changes steeper with bias increase, ϵ' reaches minimum at bias 300 Oe higher) may arise because of following reasons. The actual shape of FMR spectrum may differ from the Lorentzian one, the width of FMR spectrum (the effective damping factor Γ) is usually bias-dependent [21]. The domain structure at the ends of the wire sections is known to be distorted [8, 19]; therefore the FMR parameters in the middle and at the ends of wire sections are different. The conductivity and domain structure across the section of the wires may be non-uniform, etc.

Using the calculated dispersion curves (Fig. 6) and applying the Fresnel's relations we can calculate the reflection and transmission spectra [23] of a sheet filled with parallel sections of fibers under study, which has complex permittivity ϵ_{mix} (Fig. 7). At the frequency corresponding to the resonance of wire length (14.4 GHz for 9 mm-long sections) $\tan \delta_\epsilon = \epsilon''/\epsilon' \approx 1$, so the transmission coefficient gradually decreases with increase of sample thickness (the interference contribution is negligible). The product of screen thickness and filling factor defines the transmission loss for a transparent screen. If the admissible loss is equal to 3 dB, then the range of attenuation control for a sample with the wires under study is about 10 dB (Fig. 7).

The regular distribution of aligned wire sections ($R_{rad} = 0$) for

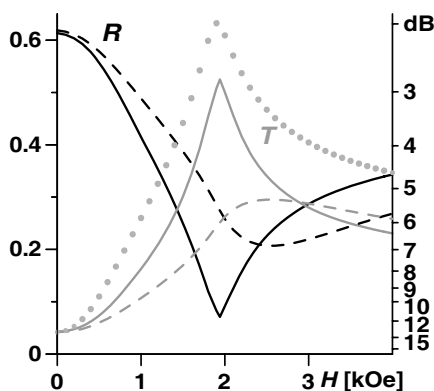


Figure 7. Power reflection (black lines) and transmission (gray lines) coefficients at 14.5 GHz as bias function of 0.4 mm thick screen filled with wire sections 8 mm-long. Solid lines correspond to the screen with aligned wires; dashed ones correspond to random oriented wires. The gray dots represent transmission in case of regular distribution of aligned wire sections in 0.25 mm thick screen.

the same attenuation of the opaque screen decreases the transmission loss in the transparent state for about 1 dB compared to a disordered anisotropic composite (see dotted and gray lines in Fig. 7).

Note that at the resonance frequency of wire sections (~ 14.4 GHz for 9 mm wires) the real part of mixture permittivity ε'_{mix} under 0–2 kOe bias is close to unity while the imaginary part is high $\varepsilon''_{mix} > 60$ and depends on the bias strength (see Fig. 5). Therefore, at the resonance frequency the composite with wire sections behaves like a resistive substance, where its equivalent resistance increases with bias, or like a composite similar to one described in [15], where the wire sections are interconnected into a continuous lattice.

The dependence of transmission on bias (Fig. 7) is similar to the dependence of equivalent resistance of a sample ρ_{mix} on bias and the dependence of wire resistance ρ_{wire} on bias (Fig. 8): $\rho_{eff} = 1/2\pi f\varepsilon_0\varepsilon''$, where ε'' of the wire is defined by Equation (4), and ε'' of a sample is defined by (1).

Comparing the effective resistance of a single wire ρ_{wire} and the equivalent resistance ρ_{mix} of the sample at 14.4 GHz we see that the ratio of wire resistance to equivalent resistance of the sample steeply increases with the bias increase up to ~ 800 Oe. Under higher bias the ratio ρ_{wire}/ρ_{mix} is almost constant. It is easy to comprehend the Γ -shape of curve by comparing it with resistance data (Fig. 8) and permittivity dispersion curves in Fig. 6. Under low bias the wire sections behave like resonant half-wave dipoles; the damping factor is small; the magnetoimpedance effect is increased proportionally to the current passing through a wire section. The current through a wire section is amplified compared to the current through a continuous wire due to dipole resonance. Under bias exceeding 1 kOe the resonance is damped, and the sections behave like resistive fibers that can be interconnected into a continuous lattice penetrating the sample (the structure measured in [15]). In this case, the ratio ρ_{wire}/ρ_{mix} is bias independent. Therefore, the effect of bias on attenuation of a sample with identical wire sections is amplified resonantly compared to the effect in the sample with continuous wires.

The above estimations of the limits of attenuation control are valid for a sample with aligned wire sections. The anisotropic composite is difficult to manufacture in practice, but the screen with random-oriented wires exhibits much lower range of attenuation control (dashed lines in Fig. 7). In this case, the maximal transparency is reached under higher bias, but the more serious drawback is that the transmission loss in a transparent state is approximately twice higher than that for a screen with aligned wires. The increased loss arises from the higher conductivity of the less magnetized wires that are inclined to bias field.

Using a similar procedure (rel. 1, 5, 6) we calculate the transmission curves at 10 and 15 GHz for the actual plane-isotropic sample with 10 mm-long wires (Fig. 4). We have a good agreement between the experimental and simulated data at 10 GHz as the FMR frequency (the frequency of δ_{\min}), and the anisotropy field H_A (5) are determined relatively accurately. The frequency of δ_{\max} and the value of minimal resistance of the wire are estimated assuming the Lorentzian shape of FMR spectrum. The discrepancy between the experimental and simulated transmission data at 15 GHz indicates that the actual FMR spectrum may be of asymmetric shape. The above mechanism of permittivity control results in the largest possible control range as it is based on the switch from the maximal to the minimal effective conductivity of the wire. The bias strength and permittivity change depend on the width and shape of FMR spectrum: the lower is the damping factor (Γ in rel. 5), the lower is the bias and the higher is the transparency control range. For a given width of FMR spectrum, the lower is the FMR frequency, the nearer are the frequencies of minimal and maximal surface impedance of the wire (Fig. 3). Therefore, the lower is the operating frequency of a composite screen, the lower is the necessary bias as the less is the required shift of FMR spectrum. For the FMR frequency of 9 GHz, the switching bias is about 2 kOe, while for ~ 2 GHz the switching bias is about $500 \div 700$ Oe [15].

The maximal control range can be reached only if three conditions are fulfilled simultaneously. Namely, the operating frequency must be equal to the frequency of maximal zero-bias conductivity; the wire

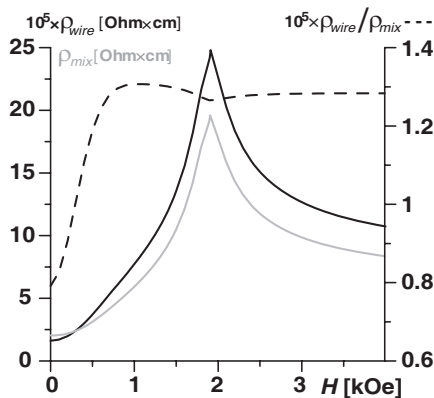


Figure 8. Effective resistance of the wire at 14.5 GHz, the equivalent resistance of the composite and their ratio as bias function presented by solid black, solid gray and dashed black lines correspondingly.

length must be equal to $\lambda/2$ at this very frequency; the maximal penetration depth δ must be close to wire diameter. The higher is the permittivity ε_h of the binder in which the wires are immersed, the shorter is the physical length of a half-wave dipole, the lower is the dipole inductance and the wider is the line of dielectric absorption. Therefore, the lower is the attenuation of the opaque screen and the lower is the range of attenuation control. It is important that if the FMR spectrum is wide or its shape is asymmetrically distorted, the maximum of effective conductivity may be reached at the frequency higher than the estimated one or may be totally absent. The case resembles the isotropic sample: the range of transparency control is smaller and the control needs stronger bias.

6. CONCLUSION

The permittivity spectra of similar composites filled with wires of permeable and impermeable metal may differ significantly. The composite filled with sections of impermeable wire has a simple Lorentzian dielectric spectrum, where the resonance frequency is defined by the section length. In case of a permeable wire, if the FMR frequency is close to the resonance length of the wire section, the permittivity spectrum has two absorption maxima because of the abrupt change of the wire impedance. This very effect explains the shape of absorption spectra obtained in [15] for a sample with a single permeable wire.

The measurements reveal that the complex permittivity of an isotropic wire-filled composite is bias-dependent at microwaves for both bias orientations relative to the polarization plane of incident wave.

At least two mechanisms of permittivity control that differ in bias strength are observed. At relatively high bias the absorption takes place due to the abrupt change of penetration depth in the vicinity of resonance of circumferential permeability. Here the bias value depends on the measurement frequency. The absorption has high intensity and is independent of the domain structure of a microwire.

The second mechanism is observed in magnetically bistable wires at bias approximately equal to the coercive field. In case of Co-based wires, the reconfiguration of domain structure takes place at bias of several Oe. The corresponding change of wire impedance (the giant magnetoimpedance) is used in magnetic sensors, though their operating frequency does not exceed several megahertz [11]. The recent reports show that the impedance change decreases with frequency, but it is observed up to 1–1.6 GHz [28, 29]. We observe the similar effect at 6 GHz (Fig. 2), but the permittivity change seems negligible for

practice. Here the magnetoimpedance coefficient $d\sigma/dH_{ext}$ is higher than in the first mechanism, but the total impedance change is much smaller. The computations [10] confirm that the maximal permittivity change due to giant magnetoimpedance effect is about 4 times lower than in case of FMR.

The widest dynamic range of attenuation control is attained with the sample filled with aligned wire sections of identical length at the frequency higher than that of FMR, namely, at the frequency where the zero-bias skin-depth is maximal. The optimal wire length is such that the zero-bias peak of absorption takes place at this very frequency. The optimal diameter of the wires is close to the maximal skin-depth. The sample thickness and filling factor define the minimal transmission loss. If the admissible loss in the transparent state is about 3 dB, then the range of attenuation control of a screen with Fe-based wires can reach 10 dB.

If the aligned wires are distributed regularly and form the ordered lattice, the screen can be thinner, and the transparency loss can be lower than in case of unordered anisotropic composite for the same range of attenuation control.

If the wire sections are oriented randomly in a screen plane, the range of attenuation control is approximately twice smaller, and the loss of in a transparent plane-isotropic screen is approximately 3 dB higher than that of a transparent screen with aligned wires. The increase of the permittivity of the media binding the wires decreases the maximal attenuation and consequently the range of attenuation control.

If the aligned wires are interconnected into a mesh, the dynamic range of attenuation control is also smaller than that for the anisotropic sample filled with wire sections of identical length, because the resonance of wire dipoles amplifies the effect of magnetoimpedance on microwave permittivity of a composite. Moreover, the range of attenuation control of a composite with continuous wires is smaller without the gain in the operating frequency band of a screen, as the band is all the same limited by the width of the FMR spectrum.

The described mechanism of attenuation control is based on the dependence of the FMR frequency on the bias strength. Therefore the controlling bias is high, and the field strength reaches $1 \div 2$ kOe. The narrower is the FMR spectrum, the lower is the required bias strength and the higher is the transparency control range.

For equal damping factors the strength of the bias switching the screen to a transparent state decreases proportionally to the decrease of the operating frequency. The situation is similar to giant magnetoimpedance: the higher is the frequency, the lower is the

magnetoimpedance coefficient. But even if the operating frequency is as low as 2 GHz, the switching bias reaches $300 \div 500$ Oe. It is about two orders higher than the bias required for the alternative mechanism related to the giant magnetoimpedance effect.

ACKNOWLEDGMENT

The authors wish to thank Prof. I. T. Iakubov for fruitful discussion and valuable remarks.

The research was partially supported by the RFBR grant No. 08-02-00830.

REFERENCES

1. Tennant, A. and B. Chambers, "Adaptive radar absorbing structure with PIN diode controlled active frequency selective surface," *Smart Mater. Struct.*, Vol. 13, 122–126, 2004.
2. Smith, F. and R. Gupta, "Principles and demonstration of multifunctional adaptive electromagnetic screen," *El. Lett.*, Vol. 39, No. 13, 967–969, 2003.
3. Schoenlinner, B., A. Abbaspour-Tamijani, L. C. Kempel, and G. M. Rebeiz, "Switchable low-loss RF MEMS Ka-band frequency-selective surface," *IEEE Trans. Microw. Theory Techn.*, Vol. 52, 2474–2481, 2004.
4. Sarkar, D., P. P. Sarkar, S. Das, and S. K. Chowdhury, "An array of stagger-tuned printed dipoles as a broadband frequency selective surface," *Microw. Opt. Techn. Lett.*, Vol. 35, 138–140, 2002.
5. Teo, P., K. A. Jose, Y. B. Gan, and V. K. Varadan, "Beam scanning of array using ferroelectric phase shifters," *El. Lett.*, Vol. 36, No. 19, 1624–1626, 2000.
6. Zhang, R., A. Barnes, K. L. Ford, B. Chambers, and P. V. Wright, "A new microwave smart window based on a poly (3,4-ethylenedioxythiophene) composite," *J. Mat. Chem.*, Vol. 3, 16–21, 2003.
7. Salahun, E., G. Tanne, and P. Queffelec, "Enhancement of design parameters for tunable ferromagnetic composite-based microwave devices: Application to filtering devices," *Digest of 2004 IEEE MTT-S Int. Microwave Symp.*, Vol. 3, 1911–1914, 2004.
8. Starostenko, S. N., K. N. Rozanov, and A. V. Osipov, "Microwave properties of composites with glass coated amorphous magnetic microwires," *JMMM*, Vol. 298, 56–64, 2006.

9. Acher, O., P.-M. Jacquart, and C. Boshier, "Magneto-impedance in glass-coated comnsib amorphous microwires," *IEEE Trans. on Magn.*, Vol. 30, No. 6, 4542–4550, 1994.
10. Makhnovskiy, D. P. and L. V. Panina, "Field dependent permittivity of composite materials containing ferromagnetic wires," *J. Appl. Phys.*, Vol. 93, No. 7, 4120–4129, 2003.
11. Antonov, A., A. Granovsky, A. Lagarkov, N. Perov, and N. Usov, "The features of GMI effect in amorphous wires at microwaves," *Physica A*, Vol. 241, 420–424, 1997.
12. Buznikov, N. A., A. S. Antonov, A. L. Dyachkov, and A. A. Rakhmanov, "Peculiarity of frequency dispersion of nonlinear magnetoimpedance in multilayer films," *Journal of Technical Physics*, Vol. 74, No. 5, 56–62, 2004 (in Russian).
13. Lagarkov, A. N., S. M. Matitsin, K. N. Rozanov, and A. K. Sarychev, "Dielectric properties of fiber-filled composites," *J. Appl. Phys.*, Vol. 84, No. 7, 3806–3818, 1998.
14. Meyer, E., H.-J. Schmitt, and H. Sewerin, "Dielektrizitätskonstante und permeabilität kunstlicher dielektrika bei 3 cm wellenlänge," *Z. Angew. Physik*, Vol. 8, No. 6, 257–263, 1956.
15. Acher, O., M. Ledieu, A.-L. Adenot, and O. Reynet, "Microwave properties of diluted composites made of magnetic wires with giant magneto-impedance effect," *IEEE Trans. on Magn.*, Vol. 39, No. 5, 3085–3090, 2003.
16. Berzhansky, V. N., V. I. Ponomarenko, V. V. Popov, and A. V. Torkunov, "Measuring the impedance of magnetic microwires in a rectangular waveguide," *Technical Physics Letters*, Vol. 31, No. 11, 959, 2005.
17. Baranov, S. A., "Permeability of an amorphous microwire in the microwave band," *Journal of Communications Technology and Electronics*, Vol. 48, No. 2, 226–228, 2003.
18. Reynet, O., A.-L. Adenot, S. Deprot, and O. Acher, "Effect of the magnetic properties of the inclusions on the high-frequency dielectric response of diluted composites," *Phys. Rev. B*, Vol. 66, 094412, 2002.
19. Vazques, M. and A. Hernando, "A soft magnetic wire for sensor applications," *Phys. D, Appl. Phys.* Vol. 29, 939–951, 1996.
20. Starostenko, S. N., A. P. Vinogradov, and S. G. Kibetz, "Performance enhancement of a dallenbach absorber due to frequency dispersion of the permittivity," *Journal of Communications Technology and Electronics*, Vol. 44, No. 7, 761–769, 1999.

21. Starostenko, S. N., K. N. Rozanov, and A. V. Osipov, "Microwave properties of composites with glass coated amorphous magnetic microwires," *MISM-2002, Book of Abstracts*, 314, 2002.
22. Starostenko, S. N., K. N. Rozanov, and A. V. Osipov, "Microwave properties of composites with chromium dioxide," *JMMM*, Vol. 300, 70–73, 2006.
23. Brehovskih, L. M., *Waves in Layered Media*, Academic Press, London, NY, 1960.
24. Lagarkov, A. N., A. K. Sarychev, T. R. Smychkovich, and A. P. Vinogradov, "Effective medium theory for microwave dielectric constant and magnetic permeability of conducting stick composites," *Journal of Electromagnetic Waves and Applications*, Vol. 6, No. 9, 1159–1176, 1992.
25. Makhnovskiy, D. P. and L. V. Panina, "Field-dependent surface impedance tensor in amorphous wires with two types of magnetic anisotropy: Helical and circumferential," *Phys. Rev. B*, Vol. 63, 144424, 2001.
26. Usov, N. A., A. S. Antonov, and A. N. Lagarkov, "Theory of giant magneto-impedance effect in amorphous wires with different types of magnetic anisotropy," *JMMM*, Vol. 185, 159–173, 1998
27. Melo, L. G. C., P. Ciureanu, and A. Yelon, "Permeability deduced from impedance measurements at microwave frequencies," *JMMM*, Vol. 249, 337–341, 2002.
28. Dominguez, M., J. M. Garcia-Beneytez, M. Vazquez, and S. E. Lo, "Microwave response of amorphous microwires: Magnetoimpedance and ferromagnetic resonance," *JMMM*, Vol. 249, 117–121, 2002.
29. Sandacci, S. I., D. P. Makhnovskiy, and L. V. Panina, "Valve-like behavior of the magnetoimpedance in the GHz range," *JMMM*, Vol. 272–276, 1855, 2004.